

# OSW-1 inhibits tumor cell proliferation and migration via uncoupling protein 2 in hepatocellular carcinoma

KAIWEN SHEN and XINGLIN JIN

Department of Hepatopancreatobiliary Surgery, The Affiliated Hospital of Yanbian University, Yanji, Jilin 133000, P.R. China

Received October 27, 2024; Accepted April 2, 2025

DOI: 10.3892/ol.2025.15107

**Abstract.** Apoptosis is one of the primary mechanisms by which anticancer drugs exert their effects. Orsaponin (OSW-1) is a natural broad-spectrum inhibitor of enterovirus replication isolated from *Ornithogalum saundersiae*. It is a specific antagonist of cholesterol-binding protein (OSBP) and OSBP-related protein 4 (ORP4). OSW-1 exhibits antitumor activity; however, its mechanism remains to be elucidated. The present study aimed to explore the cytotoxicity of OSW-1 in hepatocellular carcinoma (HCC) and its antitumor mechanisms. Gene Expression Profiling Interactive Analysis database analysis showed that uncoupling protein 2 (UCP2) expression was markedly higher in HCC tissue. Mitochondrial membrane potential and cell cycle progression in Hep3B cells were assessed by flow cytometry using JC-1 and propidium iodide staining, respectively. OSW-1 decreased mitochondrial membrane potential, induced cell cycle arrest at the G<sub>2</sub>/M phase and caused production of intracellular reactive oxygen species. Western blot and quantitative PCR determined that OSW-1 induced apoptosis in Hep3B cells by downregulating UCP2 expression. These results suggest that OSW-1 has potential as a therapeutic agent for liver cancer. Future studies should explore its effects on a broader range of HCC cell lines and *in vivo* models and investigate its molecular mechanisms and side effects.

## Introduction

According to National Cancer Center of China, there were 4.82 million new cancer cases in China in 2022, including

---

*Correspondence to:* Professor Xinglin Jin, Department of Hepatopancreatobiliary Surgery, The Affiliated Hospital of Yanbian University, 505 Aidan Road, Yanji, Jilin 133000, P.R. China  
E-mail: xljinyj@163.com

*Abbreviations:* UCP2, uncoupling protein 2; OSW-1, orsaponin; CCK-8, Cell Counting Kit-8; WB, western blot; RT-q, reverse transcription-quantitative; GEPIA, Gene Expression Profiling Interactive Analysis

*Key words:* hepatocellular carcinoma, UCP2, apoptosis, mitochondrial dysfunction, reactive oxygen species

370,000 new cases of liver cancer, making it the fourth most common cancer in China (1). Currently, the treatment of liver cancer primarily focuses on perioperative treatment, surgery and systemic drug therapy (2); however, liver cancer is often diagnosed at an advanced stage or the physical condition of the patient may preclude surgical intervention (3). Despite advances in chemotherapy and the development of targeted therapy and immunotherapy, toxic side effects remain a challenge (3).

Taxanes have potential in antitumor activity and serve an important role in cancer prevention and treatment (4). Since its isolation from *Ornithogalum saundersiae* in 1992, orsaponin (OSW-1) has demonstrated potent antitumor activity in various cancer models (5,6). However, its mechanism of action remains incompletely elucidated and the compound is challenging to synthesize, maintaining its status in the preclinical research phase (7). OSW-1 may be associated with mitochondrial function and trigger apoptosis via mitochondrial signaling pathways (8). Previous studies have reported that mitochondrial dysfunction is associated with apoptosis in hepatocellular carcinoma (HCC) cells (9,10). Uncoupling protein 2 (UCP2) regulates the production of reactive oxygen species (ROS) in mitochondria, thus influencing mitochondrial dysfunction (11). UCP2 mediates resistance to gemcitabine-induced apoptosis in HCC cell lines (12). A previous study demonstrated that OSW-1 induces necrotic apoptosis in HCC cells, primarily via the mitochondrial pathway (13). Given UCP2 role in mitochondrial-mediated chemoresistance and OSW-1's mitochondrial targeting mechanism, investigating potential interactions between UCP2 and OSW-1 could elucidate determinants of therapeutic efficacy, though direct evidence remains unconfirmed.

The present study aimed to explore the cytotoxicity of OSW-1 in HCC cells and elucidate its potential antitumor mechanisms.

## Materials and methods

*Gene Expression Profiling Interactive Analysis (GEPIA).* The updated version of GEPIA2 was utilized to analyze the differential expression of UCP2 in liver cancer, perform survival analysis, and assess its expression across different clinical stages ([gepia2.cancer-pku.cn/#analysis](http://gepia2.cancer-pku.cn/#analysis)). GEPIA2, an upgraded version of GEPIA, integrates RNA-seq data from 9,736 tumors (The Cancer Genome Atlas, TCGA) and 8,587

normal (Gene-Tissue Expression, GTEx) samples processed through the UCSC Xena standardized pipeline (<http://xena.ucsc.edu>).

**Cell lines and culture.** Human THLE-2 and Hep3B cell lines (Shanghai Fuheng Biotechnology Co., Ltd.), derived from normal human hepatocytes and HCC cells, respectively, were cultured in RPMI-1640 and Eagle's minimum essential medium supplemented with 10% fetal bovine serum and 1% penicillin and streptomycin [all (Shanghai Xiaopeng Biotechnology Co., Ltd.)]. Cells were maintained at 37°C in a humidified incubator with 5% CO<sub>2</sub>.

**OSW-1.** OSW-1 (HY-101213, CAS:145075-81-6) was purchased from MedChem Express. It was dissolved in dimethyl sulfoxide (Beijing Solarbio Science & Technology Co., Ltd.) to a concentration of 100 µg/ml and stored at -20°C.

**Cell Counting Kit-8 (CCK-8) assay.** Cell proliferation was monitored using a CCK-8 assay (Beijing Solarbio Science & Technology Co., Ltd.). The aforementioned cell lines in the logarithmic growth phase were seeded in a 96-well plate (1x10<sup>4</sup>/well) for 24 h. After treatment, CCK-8 reagent was added, followed by incubation at 37°C for 2 hours. Absorbance at 450 nm was measured using a microplate reader (Synergy Mx; BioTek; Agilent Technologies, Inc.). Data analysis was performed using SPSS (version 24.0; IBM Corp.) and samples were analyzed in quintuplicate.

**Mitochondrial membrane potential assay.** Hep3B cells in the logarithmic growth phase were incubated with OSW-1 at concentrations of 0.0, 12.5, 25.0 and 50.0 ng/ml in a 6-well plate (5x10<sup>4</sup>/well) at a constant 37 °C for 24 h. JC-1 staining solution (Beyotime Institute of Biotechnology) was added and incubated at 37°C for 25 min in the dark. Cells were then washed twice with JC-1 staining buffer. Images were captured using an inverted fluorescence microscope (Discover Echo Inc.) and analyzed with ImageJ software (Version 1.54h, National Institutes of Health). Each sample was tested in triplicate.

**Cell cycle assay.** The cell cycle was assessed using a cell cycle and apoptosis detection kit (cat. no. C1052; Beyotime Institute of Biotechnology). Following treatment aforementioned, single-cell suspensions were prepared and stained according to the manufacturer's instructions. Flow cytometry (FACSCalibur; BD Biosciences) was used to analyze (FlowJo; 10.6.2; BD) the cell cycle and triplicate experiments were performed.

**ROS assay.** According to the manufacturer's instructions (ROS Assay Kit; Beyotime Institute of Biotechnology), cells were loaded with 10 µM DCFH-DA (diluted 1:1,000 in extracellular solution) and incubated at 37°C for 20 min in the dark. After washing three times with extracellular solution to remove residual probe, ROS levels were assessed using a short-term stimulation method. Based on preliminary tests showing no detectable changes in ROS levels at lower concentrations, the drug concentration was increased 10-fold for experimental treatments. For positive controls, cells were stimulated with

Rosup (diluted 1:1,000 in PBS) at 37°C for 20-30 min to induce ROS elevation. After digesting the Hep3B cells and preparing a single-cell suspension at a concentration of 1x10<sup>6</sup>/ml, dichlorodihydrofluorescein diacetate was added and the cells were incubated at 37°C. The probe was invested and mixed every 3-5 min to allow full contact with the cells. The non-probe and Rosup positive control groups were used as the reference. The Rosup group was stimulated for 20 min and the OSW-1 group for 2 h. Flow cytometry was used to observe changes in ROS levels and each sample was analyzed in triplicate.

**Reverse transcription-quantitative (RT-q)PCR.** Hep3B cells were treated with OSW-1 as aforementioned. RNA was extracted using the TRNzol Universal method (DP424; Tiangen Biotech Co., Ltd.). Reverse transcription was performed with the FastKing cDNA First Strand Synthesis Kit (KR116; Tiangen Biotech Co., Ltd.) under the following conditions: 42°C for 15 min followed by 95°C for 3 min. Quantitative PCR was performed using a Thermo 7300 Plus PCR instrument (Thermo Fisher Scientific) with the SuperReal Fluorescence Quantitative PreMix Enhanced kit (FP205; Tiangen Biotech Co., Ltd.). Thermocycling conditions consisted of an initial denaturation at 95°C for 15 min (1 cycle), followed by 40 cycles of 95°C for 10 sec and 60°C for 26 sec. Gene expression levels were analyzed by the 2<sup>-ΔΔC<sub>q</sub></sup> method (14). Quantification was performed according to the manufacturer's protocol in the kit manual. The primer sequences were as follows: UCP2 forward, 5'-GGAGGTGGTTCGGAGATACCAA-3' and reverse, 5'-ACAATGGCATTACGAGCAACAT-3' and GAPDH forward, 5'-TCAAGGCTGAGAACGGGAAG-3' and reverse, 5'-TGGACTCCACGACGTACTCA-3'.

**Western blotting (WB).** Cells were treated as aforementioned and proteins were extracted using RIPA cell lysate (Beijing Solarbio Science & Technology Co., Ltd.) mixed with PMSF. A BCA protein assay kit (Beyotime Institute of Biotechnology) was used for protein quantification. The prepared protein samples (40 µg/lane) were separated by 12% SDS-PAGE (Beijing Solarbio Science & Technology Co., Ltd.) and transferred to nitrocellulose membranes (MilliporeSigma). The membrane was blocked in 5% skim milk at room temperature for 1 h and incubated overnight at 4°C with the following primary antibodies: BAX (1:1,000 dilution, catalogue no. WL01637; Wanleibio Co., Ltd.), Bcl-2 (1:1,000, WL01556; Wanleibio Co., Ltd.), Cleaved Caspase-3 (1:1,000, WL01992; Wanleibio Co., Ltd.), Caspase-3 (1:1,000, WL04004; Wanleibio Co., Ltd.), UCP2 (1:1,000, 11081-1-AP; Proteintech), and β-actin (1:1,000, AF7018; Affbiotech). The next day, the membrane was incubated with a fluorescent secondary antibody (IRDye 800CW goat anti-Rabbit; 1:20,000; LI-COR Biosciences) for room temperature 1 h in the dark, followed by visualization using a dual near-infrared fluorescent molecular imaging system. ImageJ was used to analyze the gray values of the bands.

**Statistical analysis.** All data are presented as the mean ± SD from three independent experimental repeats. All data were processed using SPSS 24.0 and analyzed using one-way analysis of variance followed by post hoc LSD test. Graphs were generated using the GraphPad Prism 6 software (Dotmatics).

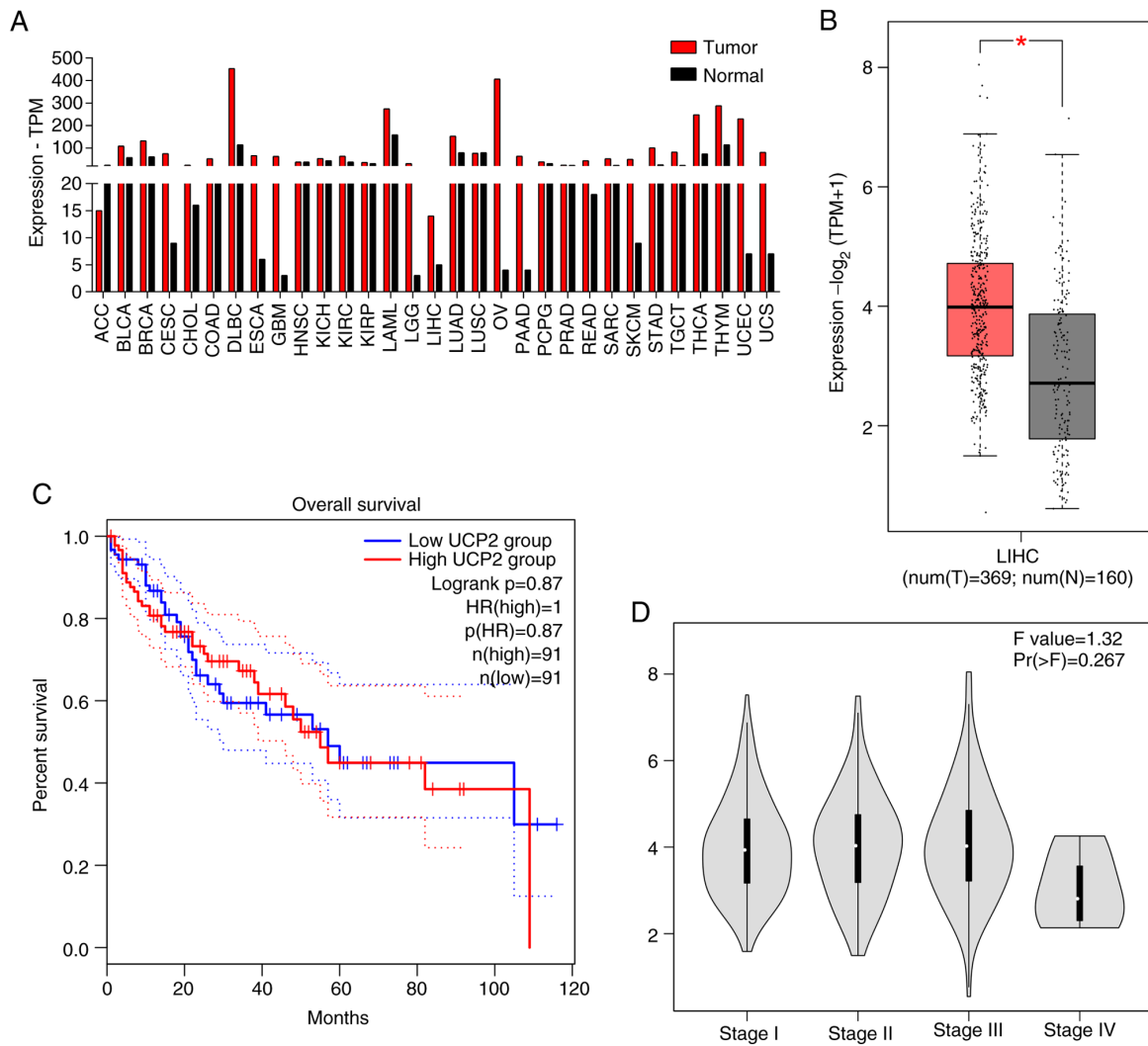


Figure 1. UCP2 expression and survival analysis in liver cancer. (A) Gene expression profile across tumor samples and paired normal tissue. (B) Box plots of UCP2 in liver cancer and normal tissue. (C) Overall survival of patients with low or high UCP2 expression in liver cancer. (D) Expression of UCP2 in liver cancer across pathological stages. \* $P<0.05$ . UCP, uncoupling protein 2; HR, hazard ratio; TPM, transcripts per million; LIHC, liver hepatocellular carcinoma.

$P<0.05$  was considered to indicate a statistically significant difference.

### Results

*UCP2 is upregulated in liver cancer.* The GEPIA database was used to assess differences in UCP2 expression between cancerous and normal human tissue. UCP2 expression was significantly higher in HCC compared with paired normal tissue (Fig. 1A). Compared with normal tissue in TCGA and GTEx data, the expression of UCP2 in liver cancer was significantly higher compared with that in normal tissues ( $P<0.05$ ; Fig. 1B). Moreover, patients with high UCP2 expression demonstrated shorter overall survival compared with those with lower expression (Fig. 1C). No significant association was found between UCP2 expression and the clinical stage of HCC (Fig. 1D).

*OSW-1 inhibits the proliferation of Hep3B cells.* To evaluate the ability of OSW-1 to inhibit cell survival, a CCK-8 assay was used. OSW-1 had a significant cytotoxic effect on Hep3B cells; however, the viability of THLE-2 cells was significantly

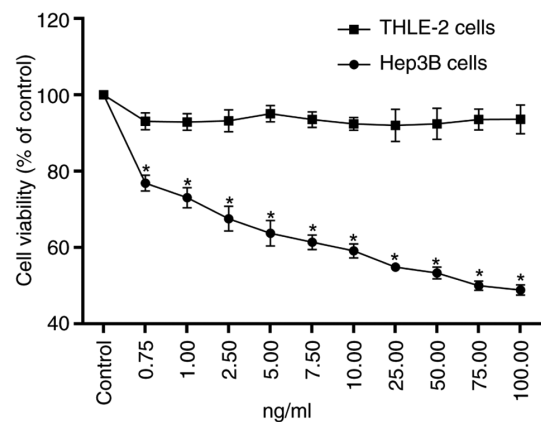


Figure 2. Proliferation of THLE-2 and Hep3B cells treated with orsaponin-1. \* $P<0.05$  vs. control.

higher compared with Hep3B cells at the same concentration ( $P<0.05$ ; Fig. 2). The half-maximal inhibitory concentration of OSW-1 against Hep3B cells was 73.97 ng/ml.

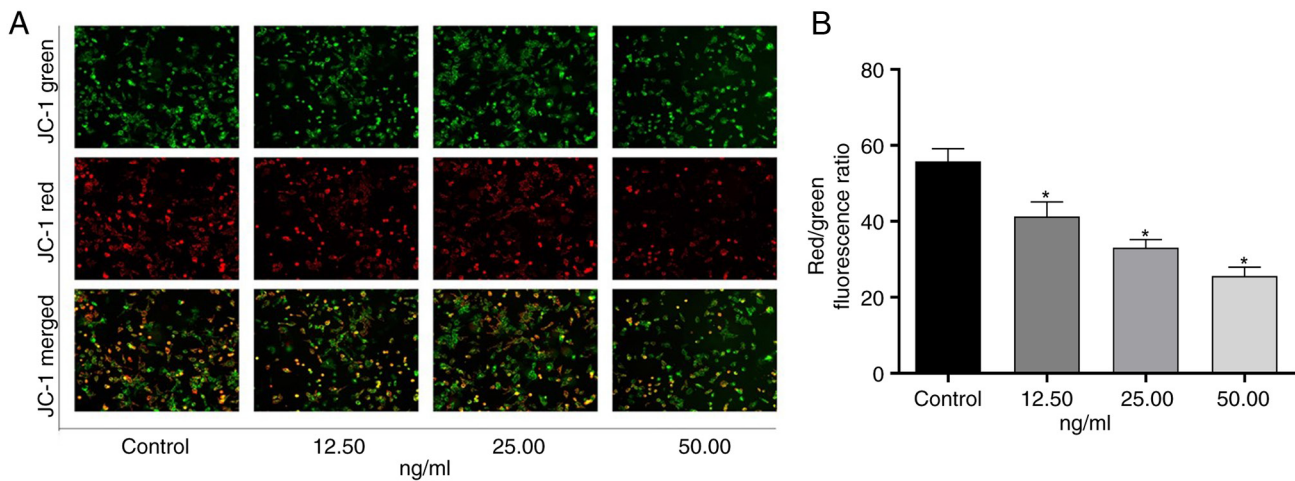


Figure 3. OSW-1 decreases the mitochondrial membrane potential. (A) Mitochondrial function of Hep3B cells treated with OSW-1. Magnification,  $\times 100$ . (B) Quantification of fluorescence ratio of red to green. \* $P < 0.05$  vs. control. OSW, orsaponin.

*OSW-1 decreases the mitochondrial membrane potential in Hep3B cells.* A decline in mitochondrial membrane potential is a hallmark of early apoptosis. To measure this, the membrane-permeable cationic dye JC-1 was used as a fluorescent probe. A decrease in mitochondrial membrane potential is indicated by the transition of JC-1 from red to green (15). OSW-1 significantly decreased the mitochondrial membrane potential in Hep3B cells in a dose-dependent manner compared with untreated controls ( $P < 0.05$ ; Fig. 3).

*OSW-1 mediates Hep3B cell cycle arrest.* OSW-1 induced significant G2/M phase arrest and partial S phase accumulation in Hep3B cells, concurrent with reduced G0/G1 population. ( $P < 0.05$ ; Fig. 4).

*Effect of OSW-1 on ROS in Hep3B cells.* OSW-1 markedly increased intracellular ROS levels (Fig. 5A). Compared with the control group, 125, 250, and 500 ng/ml OSW-1 treatments induced significant increases in M2 gated cells (%) ( $P < 0.05$ ; Fig. 5B).

*OSW-1 induces apoptosis in Hep3B cells via UCP2.* To investigate how OSW-1 induces apoptosis in Hep3B cells, WB and RT-qPCR were performed to assess UCP2 protein and mRNA expression, respectively. RT-qPCR analysis demonstrated that the expression of UCP2 mRNA decreased in a dose-dependent manner with increasing OSW-1 concentration. Compared with the control group, 12.5, 25.00, and 50.00 ng/ml OSW-1 reduced UCP2 mRNA ( $P < 0.05$ ; Fig. 6B). Similarly, WB (Fig. 6C) demonstrated that the expression of UCP2 decreased with an increase in OSW-1 concentration ( $P < 0.05$ ). The protein expression of UCP2 decreased with longer treatment times at 12.5 ng/ml OSW-1 (Fig. 6A) and the 48- and 72-h groups were significantly decreased compared with the untreated control group ( $P < 0.05$ ). Compared with the control, Bcl-2 was downregulated, Bax was upregulated and the Bax/Bcl-2 ratio was significantly increased with OSW-1 treatment. In addition, cleaved-caspase3/caspase3 levels were significantly increased compared with the control ( $P < 0.05$ ).

## Discussion

OSW-1 was first isolated from the bulbs of *O. saundersiae* by Kubo *et al* (16) in 1992. Researchers have studied OSW-1 in-depth and have reported notable anticancer activity across several cancer types (17,18). OSW-1 is considered a promising anticancer drug due to its low toxicity in non-malignant cells; however, its clinical application remains limited due to its unclear anticancer mechanisms and low yield (19). In the present study, the cytotoxicity of OSW-1 in HCC cells and normal hepatocytes was assessed. OSW-1 exhibited low toxicity in normal hepatocytes and significant toxicity in HCC cells.

There is an association between mitochondrial dysfunction and liver cancer (20). Numerous studies have reported that UCP2 affects mitochondrial dysfunction and ROS production (21,22). Additionally, miR-214 suppresses HCC progression and reverses chemoresistance by targeting UCP2 expression to regulate ROS homeostasis and apoptosis. (23). In the present study, using GEPIA database analysis, the expression of UCP2 in HCC was significantly higher compared with normal tissue. Therefore, UCP2 may serve an important role in liver cancer progression. The lack of significance between the clinical stages may be due to a small sample size.

Apoptosis is one of the primary mechanisms by which anticancer drugs exert their effects. Iguchi *et al* (24) demonstrated that OSW-1 induces apoptosis in HL-60 cells via a mitochondria-independent signaling pathway, while Wu *et al* (25) reported that OSW-1 suppresses triple-negative breast cancer growth and metastasis by inducing  $Ca^{2+}$ -dependent mitochondrial apoptosis and cytoprotective autophagy via PI3K/Akt-mTOR pathway inhibition, while synergizing with chemotherapy agents. Therefore, it was hypothesized that apoptosis may be a key mechanism of OSW-1-induced tumor cell death. Apoptosis-associated proteins were evaluated; OSW-1 downregulated the expression of Bcl-2, upregulated the expression of Bax, and increased Bax/Bcl-2 and cleaved-caspase3/caspase3 ratios, indicating, apoptosis in Hep3B cells treated with OSW-1 was markedly increased.

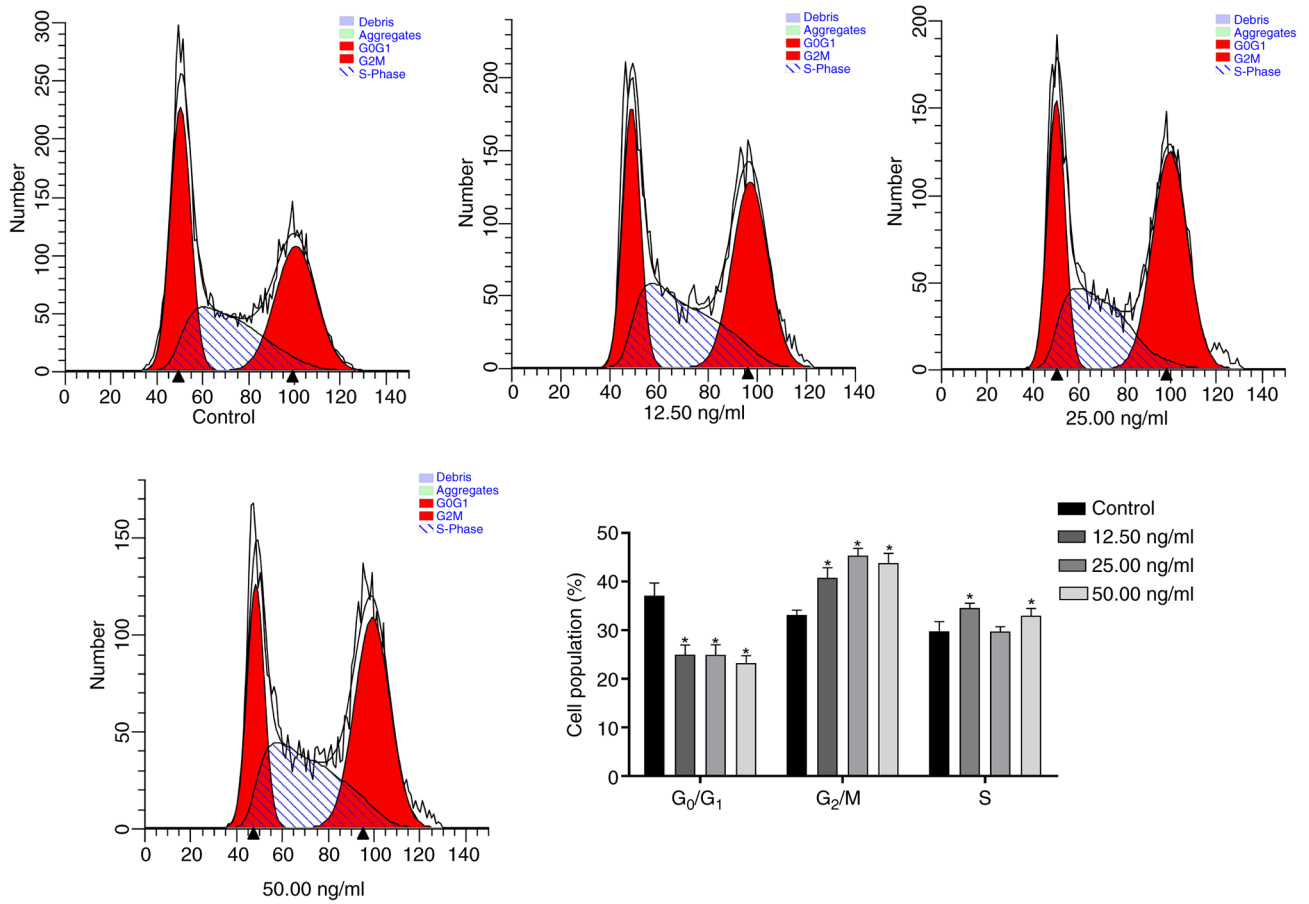


Figure 4. Effects of OSW-1 on the Hep3B cell cycle progression. \*P<0.05 vs. control.

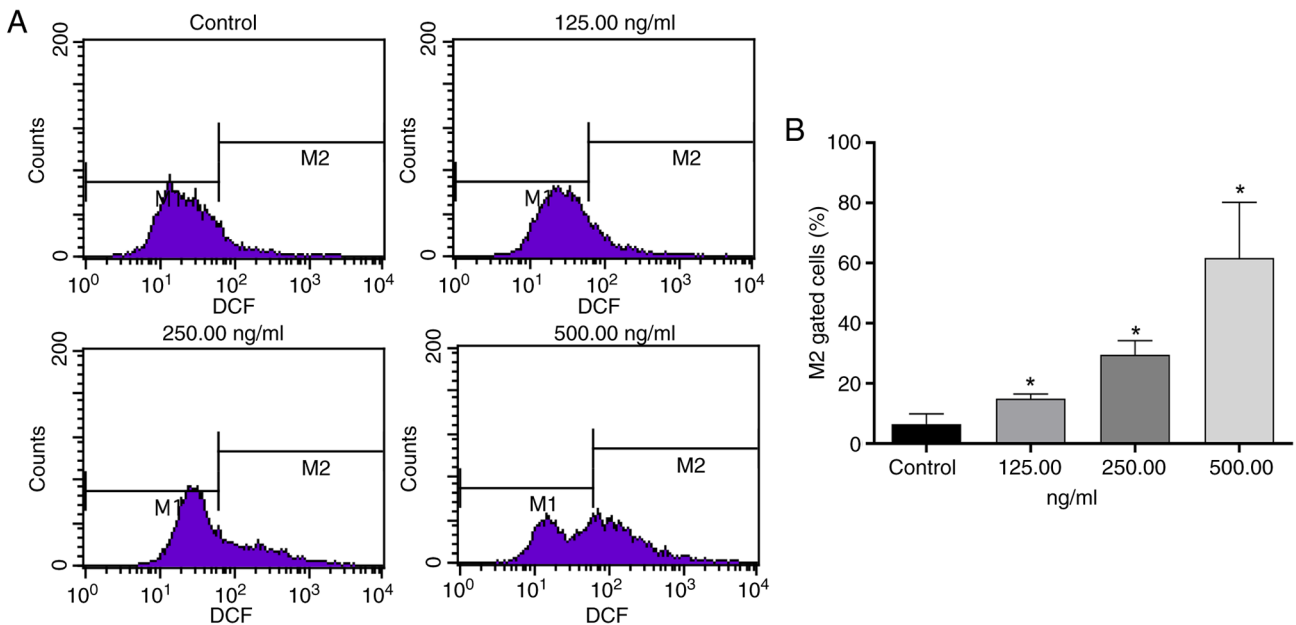


Figure 5. Effects of OSW-1 on ROS levels in Hep3B cells. (A) Intracellular ROS levels were measured using flow cytometry. (B) Proportion of M2 gated cells in each group. \*P<0.05 vs. control. ROS, reactive oxygen species.

UCP2 can resist inflammation and apoptosis in mice with sepsis-associated encephalopathy by affecting mitochondrial dysfunction and ROS accumulation (26). The UCP2-associated

mitochondrial pathway is involved in orthoxylin-induced apoptosis in human colon cancer cells (27). Therefore, OSW-1 may target and inhibit highly expressed UCP2 in HCC,

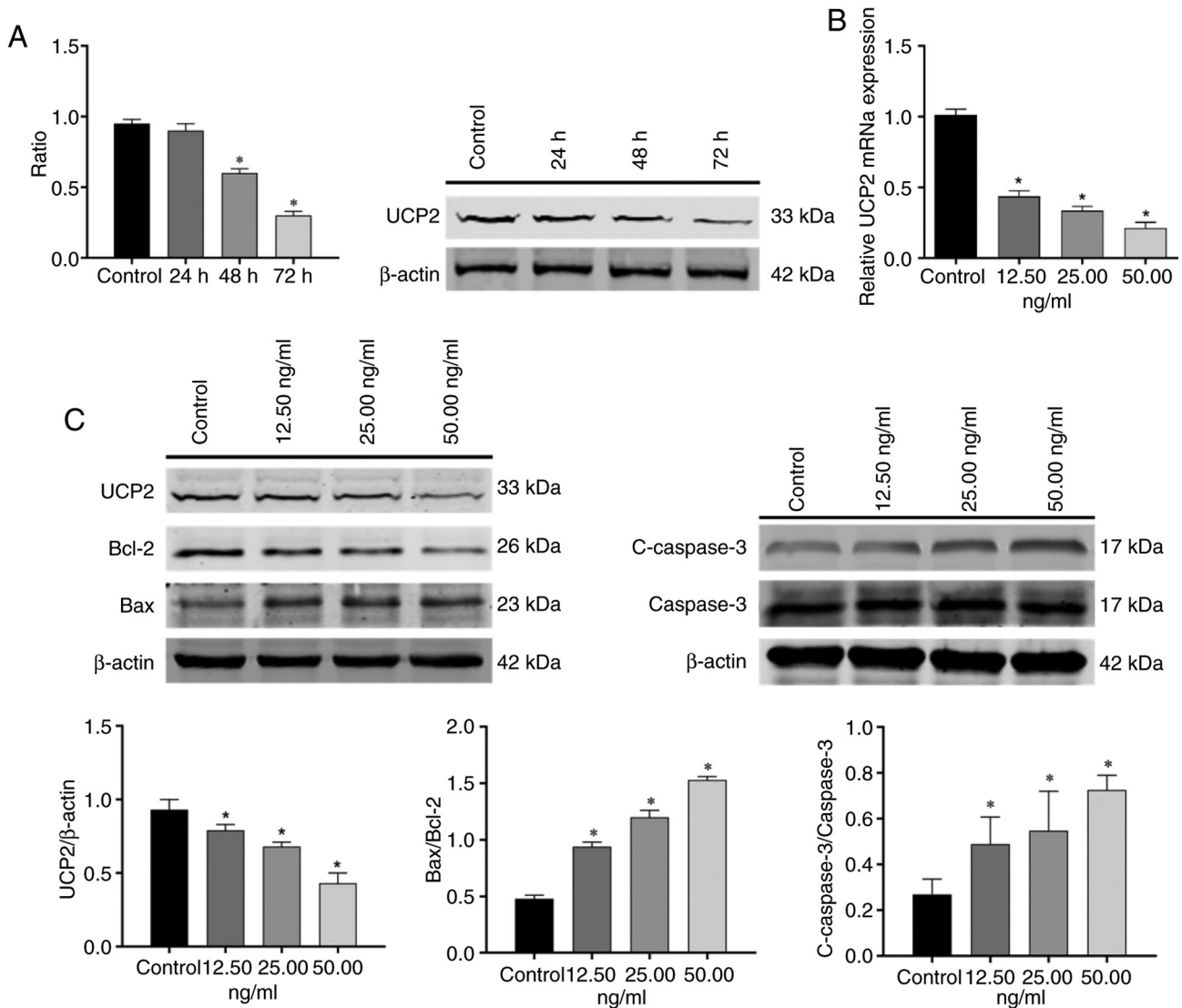


Figure 6. OSW-1 induces apoptosis of liver cancer cells via UCP2. (A) mRNA expression of UCP2 was determined by reverse transcription-quantitative PCR. (B) UCP2 protein expression following 12.5 ng/ml OSW-1 treatment at different time points. \* $P < 0.05$  vs. control. (C) Western blotting of apoptosis-associated proteins following OSW-1 treatment. UCP2, uncoupling protein 2; OSW, orsaponin.

disrupting its regulation of mitochondrial ROS homeostasis, leading to ROS accumulation and mitochondrial dysfunction. In the present study, the expression of UCP2 decreased with an increase in OSW-1 concentration and time, demonstrating an association between UCP2 and OSW-1. Here, membrane potential decreased with an increase in the concentration of OSW-1. This unexpected reduction in membrane potential, despite decreased UCP2 expression, suggests that OSW-1 may exert additional effects on mitochondrial ion homeostasis. UCP2, a proton transporter, is an inner mitochondrial membrane carrier protein that can induce proton leakage and dissipate the proton gradient, which may be an important mechanism for controlling mitochondrial ROS production by adjusting the mitochondrial membrane potential (28-31).

Previous studies have demonstrated that changes in the cell cycle can affect the occurrence and process of apoptosis and that cell cycle arrest and apoptosis serve antitumor roles (32,33). Abusaliya *et al* (34) demonstrated that prunetin induces cell cycle arrest and intrinsic apoptosis in Hep3B cells via inhibition of Akt/mTOR and activation of p38/MAPK signaling. In the

present study, flow cytometry demonstrated that the proportion of Hep3B cells treated with OSW-1 was significantly increased in the G<sub>2</sub>/M phase. This was similar to the findings of Liu *et al* (35), who reported that silencing of UCP2 sensitizes HeLa cells to radiation-induced DNA damage, leading to increased apoptosis, G<sub>2</sub>/M cell cycle arrest and increased mitochondrial ROS production. UCP2 can inhibit the production of mitochondrial ROS, thereby alleviating oxidative stress-induced apoptosis (36,37). In the present study, the concentration of ROS increased with increasing OSW-1 concentration. Furthermore, UCP2 expression decreased with increasing OSW-1 concentration. UCP2 is a molecular sensor and inhibitor of mitochondrial ROS production and serves an important role in regulating apoptosis in different cell systems (38).

The present study has some limitations, such as exclusive use of Hep3B cells. HCC cell lines vary in genetic makeup and biological behavior, so the present findings may not apply to other cell lines. This restricts full understanding of effects of OSW-1 on HCC. Future research should involve multiple cell lines to confirm if the effects are consistent. Additionally, the

specific molecular pathways by which OSW-1 affects UCP2 remain unclear, requiring further investigation. Notably, the present study did not account for patient comorbidities or treatment differences, which may confound the association between UCP2 expression and survival outcomes. Comorbid conditions may independently alter mitochondrial ROS dynamics, while prior therapy might modulate UCP2 levels, potentially obscuring the impact of UCP2 expression on prognosis and survival. To address this, future studies should integrate clinical metadata into survival analyses, stratify cohorts by treatment history and employ comorbidity-mimicking models to determine how these factors influence OSW-1 efficacy and UCP2-associated mechanisms. Finally, the present study did not address the potential side effects of OSW-1 in normal tissue, which is key for its therapeutic application in cancer treatment.

In conclusion, OSW-1 promotes apoptosis in Hep3B cells, potentially via the modulation of UCP2 expression. These findings provide insight into the potential of OSW-1 as a therapeutic agent for liver cancer. Future studies should explore the effects of OSW-1 across a range of HCC cell lines and *in vivo* models to validate its therapeutic potential. Additionally, investigating the molecular mechanisms of the interaction between OSW-1 and UCP2 and its potential side effects on normal tissue is essential for clinical application.

#### Acknowledgements

Not applicable.

#### Funding

The present study was supported by the National Natural Science Foundation of China (grant no. 8216140392).

#### Availability of data and materials

The data generated in the present study may be requested from the corresponding author.

#### Authors' contributions

KS performed data analysis and wrote the manuscript. XJ and KS designed the study and confirm the authenticity of all the raw data. Both authors have read and approved the final manuscript.

#### Ethics approval and consent to participate

The present study was approved by the Ethics Committee of the Affiliated Hospital of Yanbian University. The present study complied with the principles of the Declaration of Helsinki and the Ethical Review of Biomedical Research Involving Human Beings.

#### Patient consent for publication

Not applicable.

#### Competing interests

The authors declare that they have no competing interests.

#### References

- Han B, Zheng R, Zeng H, Wang S, Sun K, Chen R, Li L, Wei W and He J: Cancer incidence and mortality in China, 2022. *J Natl Cancer Cent* 4: 47-53, 2024.
- Wang X, Meng F and Mao J: Progress of natural sesquiterpenoids in the treatment of hepatocellular carcinoma. *Front Oncol* 14: 1445222, 2024.
- Wang B, Hao X, Yan J, Li X, Zhao M and Han T: A bibliometric analysis of immune-related adverse events in cancer patients and a meta-analysis of immune-related adverse events in patients with hepatocellular carcinoma. *J Transl Int Med* 12: 225-243, 2024.
- Hadkar VM, Mohanty C and Selvaraj CI: Biopolymeric nano-carriers in cancer therapy: Unleashing the potency of bioactive anticancer compounds for enhancing drug delivery. *RSC Adv* 14: 25149-25173, 2024.
- Yao Y, Chen Y, Yao T, Li C, Li S and Wang N: Anticancer effects of OSW-1 on colorectal cancer cells via the ROS/NLRP3/caspase-1 pyroptosis signaling pathway. *Int Immunopharmacol* 148: 114054, 2025.
- Zhan Z, Liu Z, Zhang C, Gao H, Lai J, Chen Y and Huang H: Anticancer effects of OSW-1 on glioma cells via regulation of the PI3K/AKT signal pathway: A network pharmacology approach and experimental validation *in vitro* and *in vivo*. *Front Pharmacol* 13: 967141, 2022.
- Zhan Z, Liu Z, Lai J, Zhang C, Chen Y and Huang H: Anticancer effects and mechanisms of OSW-1 isolated from *Ornithogalum saundersiae*: A review. *Front Oncol* 11: 747718, 2021.
- Garcia-Prieto C, Riaz Ahmed KB, Chen Z, Zhou Y, Hammoudi N, Kang Y, Lou C, Mei Y, Jin Z and Huang P: Effective killing of leukemia cells by the natural product OSW-1 through disruption of cellular calcium homeostasis. *J Biol Chem* 288: 3240-3250, 2013.
- Lee HY, Nga HT, Tian J and Yi HS: Mitochondrial metabolic signatures in hepatocellular carcinoma. *Cells* 10: 1901, 2021.
- Zeng L, Zhu L, Fu S, Li Y and Hu K: Mitochondrial dysfunction-molecular mechanisms and potential treatment approaches of hepatocellular carcinoma. *Mol Cell Biochem* 480: 2131-2142, 2025.
- Szewczyk A, Jarmuszkiewicz W, Koziel A, Sobieraj I, Nobik W, Lukasiak A, Skup A, Bednarczyk P, Drabarek B, Dymkowska D, *et al*: Mitochondrial mechanisms of endothelial dysfunction. *Pharmacol Rep* 67: 704-710, 2015.
- Yu G, Liu J, Xu K and Dong J: Uncoupling protein 2 mediates resistance to gemcitabine-induced apoptosis in hepatocellular carcinoma cell lines. *Biosci Rep* 35: e00231, 2015.
- Jin J, Jin X, Qian C, Ruan Y and Huang H: Signaling network of OSW-1-induced apoptosis and necroptosis in hepatocellular carcinoma. *Mol Med Rep* 7: 1646-1650, 2013.
- Livak KJ and Schmittgen TD: Analysis of relative gene expression data using real-time quantitative PCR and the 2(-Delta Delta C(T)) method. *Methods* 25: 402-408, 2001.
- Perelman A, Wachtel C, Cohen M, Haupt S, Shapiro H and Tzur A: JC-1: Alternative excitation wavelengths facilitate mitochondrial membrane potential cytometry. *Cell Death Dis* 22: e430, 2012.
- Kubo S, Mimaki Y, Terao M, Sashida Y, Nikaido T and Ohmoto T: Acylated cholestane glycosides from the bulbs of *Ornithogalum saundersiae*. *Phytochemistry* 31: 3969-3973, 1992.
- Ding X, Li Y, Li J and Yin Y: OSW-1 inhibits tumor growth and metastasis by NFATc2 on triple-negative breast cancer. *Cancer Med* 9: 5558-5569, 2020.
- Wang N, Li CY, Yao TF, Kang XD and Guo HS: OSW-1 triggers necroptosis in colorectal cancer cells through the RIPK1/RIPK3/MLKL signaling pathway facilitated by the RIPK1-p62/SQSTM1 complex. *World J Gastroenterol* 30: 2155-2174, 2024.
- Zhang Y, Fang F, Fan K, Zhang Y, Zhang J, Guo H, Yu P and Ma J: Effective cytotoxic activity of OSW-1 on colon cancer by inducing apoptosis *in vitro* and *in vivo*. *Oncol Rep* 37: 3509-3519, 2017.
- Zhang C, Zhao Y, Yu M, Qin J, Ye B and Wang Q: Mitochondrial dysfunction and chronic liver disease. *Curr Issues Mol Biol* 44: 3156-3165, 2022.
- Serviddio G, Bellanti F, Tamborra R, Rollo T, Capitanio N, Romano AD, Sastre J, Vendemiale G and Altomare E: Uncoupling protein-2 (UCP2) induces mitochondrial proton leak and increases susceptibility of non-alcoholic steatohepatitis (NASH) liver to ischaemia-reperfusion injury. *Gut* 57: 957-965, 2008.

22. Nesci S and Rubattu SL: UCP2, a member of the mitochondrial uncoupling proteins: An overview from physiological to pathological roles. *Biomedicines* 12: 1307, 2024.
23. Yu G, Wang J, Xu K and Dong J: Dynamic regulation of uncoupling protein 2 expression by microRNA-214 in hepatocellular carcinoma. *Biosci Rep* 36: e00335, 2016.
24. Iguchi T, Kuroda M, Naito R, Watanabe T, Matsuo Y, Yokosuka A and Mimaki Y: Cholestane glycosides from *Ornithogalum saundersiae* bulbs and the induction of apoptosis in HL-60 cells by OSW-1 through a mitochondrial-independent signaling pathway. *J Nat Med* 73: 131-145, 2019.
25. Wu M, Huang Q, Liao M, Wu X, Xi H, Ma H, Li S, Zhang Y and Xia Y: OSW-1 induces apoptosis and cyto-protective autophagy, and synergizes with chemotherapy on triple negative breast cancer metastasis. *Cell Oncol (Dordr)* 45: 1255-1275, 2022.
26. Zhao P, Li X, Yang Q, Lu Y, Wang G, Yang H, Dong J and Zhang H: Malvidin alleviates mitochondrial dysfunction and ROS accumulation through activating AMPK- $\alpha$ /UCP2 axis, thereby resisting inflammation and apoptosis in SAE mice. *Front Pharmacol* 13: 1038802, 2023.
27. Qiao C, Wei L, Dai Q, Zhou Y, Yin Q, Li Z, Xiao Y, Guo Q and Lu N: UCP2-related mitochondrial pathway participates in oroxylin A-induced apoptosis in human colon cancer cells. *J Cell Physiol* 230: 1054-1063, 2015.
28. Yu J, Shi L, Lin W, Lu B and Zhao Y: UCP2 promotes proliferation and chemoresistance through regulating the NF- $\kappa$ B/ $\beta$ -catenin axis and mitochondrial ROS in gallbladder cancer. *Biochem Pharmacol* 172: 113745, 2020.
29. El-Khoury TG, Bahr GM and Echtay KS: Muramyl-dipeptide-induced mitochondrial proton leak in macrophages is associated with upregulation of uncoupling protein 2 and the production of reactive oxygen and reactive nitrogen species. *FEBS J* 278: 3054-3064, 2011.
30. El Hoss S, Bahr GM and Echtay KS: Lopimune-induced mitochondrial toxicity is attenuated by increased uncoupling protein-2 level in treated mouse hepatocytes. *Biochem J* 468: 401-407, 2015.
31. Kukat A, Dogan SA, Edgar D, Mourier A, Jacoby C, Maiti P, Mauer J, Becker C, Senft K, Wibom R, *et al*: Loss of UCP2 attenuates mitochondrial dysfunction without altering ROS production and uncoupling activity. *PLoS Genet* 10: e1004385, 2014.
32. Morihara H, Yamada T, Tona Y, Akasaka M, Okuyama H, Chatani N, Shinonome S, Ueyama A and Kuwabara K: Anti-CTLA-4 treatment suppresses hepatocellular carcinoma growth through Th1-mediated cell cycle arrest and apoptosis. *PLoS One* 19: e0305984, 2024
33. Ni K, Li ZL, Hu ZY and Hong L: Antitumor effect of apcin on endometrial carcinoma via p21-mediated cell cycle arrest and apoptosis. *Curr Med Sci* 44: 623-632, 2024.
34. Abusaliya A, Jeong SH, Bhosale PB, Kim HH, Park MY, Kim E, Won CK, Park KI, Heo JD, Kim HW, *et al*: Mechanistic action of cell cycle arrest and intrinsic apoptosis via inhibiting Akt/mTOR and activation of p38-MAPK signaling pathways in hep3B liver cancer cells by prunetin-a flavonoid with therapeutic potential. *Nutrients* 15: 3407, 2023.
35. Liu CH, Huang ZH, Dong XY, Zhang XQ, Li YH, Zhao G, Sun BS and Shen YN: Inhibition of uncoupling protein 2 enhances the radiosensitivity of cervical cancer cells by promoting the production of reactive oxygen specie. *Oxid Med Cell Longev* 2011: 1841783, 2021.
36. Hu C, Zhang X, Wei W, Zhang N, Wu H, Ma Z, Li L, Deng W and Tang Q: Matrine attenuates oxidative stress and cardiomyocyte apoptosis in doxorubicin-induced cardiotoxicity via maintaining AMPK $\alpha$ /UCP2 pathway. *Acta Pharm Sin B* 9: 690-701, 2019.
37. Lou J, Wang Y, Wang X and Jiang Y: Uncoupling protein 2 regulates palmitic acid-induced hepatoma cell autophagy. *Biomed Res Int* 2014: 810401, 2014.
38. Derdak Z, Garcia TA and Baffy G: Detection of uncoupling protein-2 (UCP2) as a mitochondrial modulator of apoptosis. *Methods Mol Biol* 559: 205-217, 2009.



Copyright © 2025 Shen and Jin. This work is licensed under a Creative Commons Attribution-NonCommercial-NoDerivatives 4.0 International (CC BY-NC-ND 4.0) License.